Proceedings of the 2nd International Conference on Computational Heat and Mass Transfer
COPPE/UFRJ – Federal University of Rio de Janeiro, Brazil, October 22-26, 2001

NUMERICAL SIMULATION OF THE EXPERIMENTAL ICP AND MICROWAVE PLASMA TORCHES WITH THE REVERSE VORTEX STABILIZATION

ALEXANDER GUTSOL[*], ALEXANDRE CHIROKOV[†], ALEXANDER FRIDMAN[‡] AND WILLIAM WOREK[§]

Abstract. Recently invented method of the Reverse-Vortex Stabilization (RVS) of plasma is compared with the traditional Forward-Vortex Stabilization (FVS) of plasma. FLUENT programming package was used for numerical simulations of electrodeless plasma torches – Radio-Frequency (RF) with Inductively Coupled Plasma (ICP) and Micro-Wave (MW). Experimental calorimetric investigations and numerical simulations were carried out to compare energetic characteristics of MW and RF inductive plasma torches with RVS and FVS. Results of investigations show that RVS is very promising for different plasma technology applications. A discrepancy between experimental and calculated results is small enough to conclude that the energy losses might be reliably predicted on the design stage of electrodeless plasma torches with the both types of vortex stabilization.

Keywords: Reverse vortex, Plasma stabilization, Inductively coupled plasma, Microwave plasma.

1. Introduction. Plasma sources are probably the most powerful system with relatively small dimensions and heat transfer problems in such system are extremely important. One of the common methods for plasma-wall insulation used in plasma sources is the vortex flow. Due to buoyancy in the centrifugal force field a hot plasma fluid is fixed on the system axis. In the usual vortex method of plasma stabilization and insulation the vortex generator is placed upstream relative to the electric discharge and the outlet of the plasma jet is directed to the opposite side, so we named this method as Forward-Vortex Stabilization (FVS). In such systems with intensive flow rotation the pressure minimum on the axis near the vortex generator is deeper than that downstream. As a result a central reverse flow forms and transfers the energy from the center of the vortex-stabilized plasma upstream, and a significant part of this energy is absorbed by the plasma torch walls and becomes lost. An idea of the Reverse-Vortex Stabilization (RVS) is to direct an outlet of the plasma jet along the axis to the swirl generator side (Gutsol, 1997a; Kalinnikov and Gutsol, 1997). In this case the plasma gas comes into discharge zone from all sides except the outlet side and no significant recirculation zone is formed (Gutsol and Bakken, 1998).

Experimental calorimetric investigations were carried out to compare energetic characteristics of MW (Kalinnikov and Gutsol, 1997) and RF (Gutsol et al, 1999a) inductive plasma torches with RVS and FVS. It was found that in experimental MW plasma torch with RVS the heat loses are 4 - 7 % depending on gas consumption. In the industrial MW plasma torch with FVS the heat loses are 26 - 42 %. Total power of MW plasma torch was about 3.5 kW. When we replaced FVS by RVS for argon inductively coupled plasma (ICP) torch with plate power up to 60 kW the increase of heat efficiency was not so impressive due to high radiation of ICP and specific circular geometry of heat generation zone. Nevertheless the RVS ICP torch has some important advantageous in comparison with all traditional ICP torches – less gas consumption which is important for analytical applications. The second feature is a possibility to inject an additional axial flow from the closed end of the system without substantially disrupting the flow pattern. This gives opportunity to treat large quantities of material (gaseous or disperse) inside the active zone of plasma and the treated products should not interact with the plasma torch wall significantly.

FLUENT programming package was used for numerical simulations of these electrodeless plasma torches (Gutsol and Bakken, 1998; Gutsol et al, 1999b). Numerical simulations in cited paper were not self-consistent. Electromagnetic part of the problems solved separately based on the experimental data about the discharge geometry. Though the results of investigations showed that RVS is very promising for different plasma technology applications, it was not possible to make reliable design of new systems without further development of numerical model. In this paper we present results of simulation performed with the help of developed self-consistent model, which allow numerical modeling of electrodeless plasma system for following design.

2. Microwave Plasma Torch: Experiments and Simulation. Experiments were made with a microwave (MW) plasma generator with a MW power input up to 5 kW. This plasma torch is a part of an experimental set-up for treatment of inorganic salt solutions (Gutsol, 1995). A sketch of the MW plasma torch with the supposed flow patterns of gas and plasma is shown in Fig. 1. The quartz discharge tube (1) (inner diameter 44 mm, length about 140 mm) passes perpendicularly through two wave-guides (90×45 mm^2, not shown), which supply the H_{10} mode of the MW

University of Illinois at Chicago, Department of Mechanical Engineering – MC 251, 842 West Taylor Street, Chicago, Illinois 60607-7022, U.S.A.
[*] agutsol@uic.edu
[†] cirokov@uic.edu
[‡] afridman@uic.edu
[§] wworek@uic.edu

energy (frequency 2.4 GHz) from two magnetrons. In the conventional FVS scheme (Fig. 1a) the plasma gas (air or nitrogen) enters the discharge chamber through four inlet openings of the original tangential vortex generator (2), resulting in stabilization of the plasma (30 on the axis of the quartz tube 1 by the strong rotation of the gas. In the experimental plasma-chemical set-up the MW plasma torch is joined to the uncooled massive steel reactor (4) by an uncooled connecting steel cone (5).

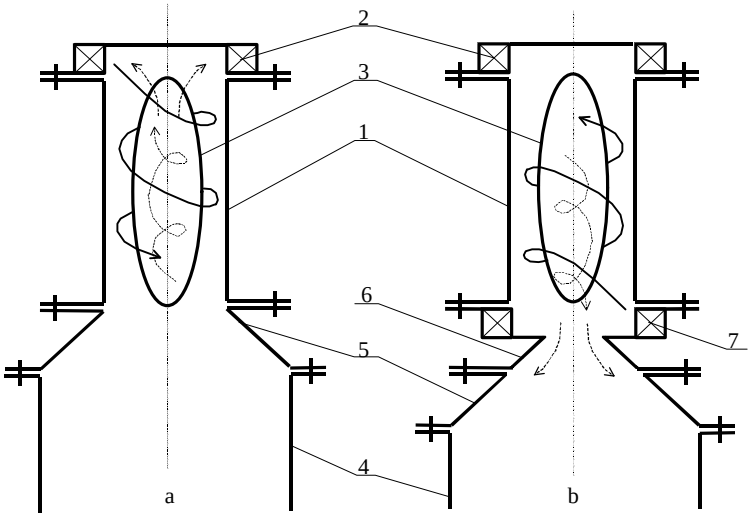

Fig. 1: Scheme of the MW plasma torches with supposed flow patterns of gas and plasma. (a) – FVS scheme with flow patterns for conventional vortex plasma stabilization; (b) – RVS scheme with flow patterns for reverse vortex plasma stabilization. 1 - cylindrical quartz tube; 2 - original swirl generator; 3 - plasma; 4 - plasma chemical reactor; 5 - connecting cone; 6 - water-cooled diaphragm; 7 - additional swirl generator.

For experiments with RVS (Fig. 1b) an additional vortex generator (7) with a water-cooled diaphragm (6) (diameter 26 mm) was installed between the quartz tube and connecting cone. Calorimetric and electrical measurements permitted to determine the MW power input W_p into the discharge and the heat losses W_t to the water-cooled parts of the plasma torch. Unfortunately it is not possible to use water cooling for the quartz tube of the MW plasma torch, but as this tube is surrounded by the water-cooled parts of the plasma torch almost on all sides, it was supposed that practically all the heat from the quartz tube ends up in the cooling system due to convection.

The experimental results are presented in Fig. 2 (dots with full curves) in dependence on J - the energy input into the discharge per unit mass of plasma gas consumption. The power input was around 3.5 kW and varies a little due to the fact that changing the gas flow conditions also influences the discharge conditions. The dots of curve (1) were obtained for the FVS scheme (Fig. 1a) *without* the diaphragm and with the plasma-chemical reactor. Curve (2) corresponds to the same scheme, but *with* the diaphragm. Curve (3) corresponds to the RVS scheme (Fig. 1b) with the reactor. As the heat flux to the plasma torch walls from the reactor was significant, two additional series of experiments were made. The reactor was removed, the plasma torch was turned upside-down, and a hot plasma flow was directed upwards into ambient air. As the heat losses in the FVS scheme without the diaphragm were extremely large for all energy inputs, only the "new" scheme (Fig. 1b) was used in the additional experiments. Plasma gas might be supplied through the original vortex generator (2) (Fig. 1) for realizing the conventional FVS scheme, or through the additional vortex chamber (7) (Fig. 1) for realizing the *reverse vortex* scheme of plasma stabilization. Curves (2') and (3') (Fig. 2) correspond to these two cases.

The experimental investigation showed that if the plasma was stabilized by the conventional vortex flow the energy loss to the plasma torch walls might exceed 30 %. With the RVS the energy loss was only about 5 %. The heat loss in a simple system of this type corresponds to the low heat loss in plasma generators with a porous discharge chamber, which, however, is very complex end expensive to manufacture. More over, if the RVS is used, almost all the plasma forming gas should pass through the discharge zone. As the axial velocity in the "top" region of the reverse vortex should be quite low, discharge stability problems should not occur. As the flow direction should be constant throughout the axial region, it seems possible to inject additional gas or particles into the "top" of the reverse vortex. Tests with ZrO_2+Y_2O_3 powder were made in the described MW facility. The introduction of the powder into the "top" of plasma torch with the RVS plasma ensures melting and spheroidization of particles up to 100 μm.

The numerical simulations of the MW plasma torch were made using the fluid flow and heat transfer simulation program FLUENT. In the 2D axisymmetric geometry the conservation equations for mass, energy and radial, axial and azimuthal momentum were solved simultaneously. To account for turbulence the Reynolds Stress Model (RSM) was used. This model involves calculation of the individual Reynolds stresses and is more suitable for rotating flows than the usual k-ε turbulence model. In the near-wall region the program used the logarithmic law for velocity. The law-of-

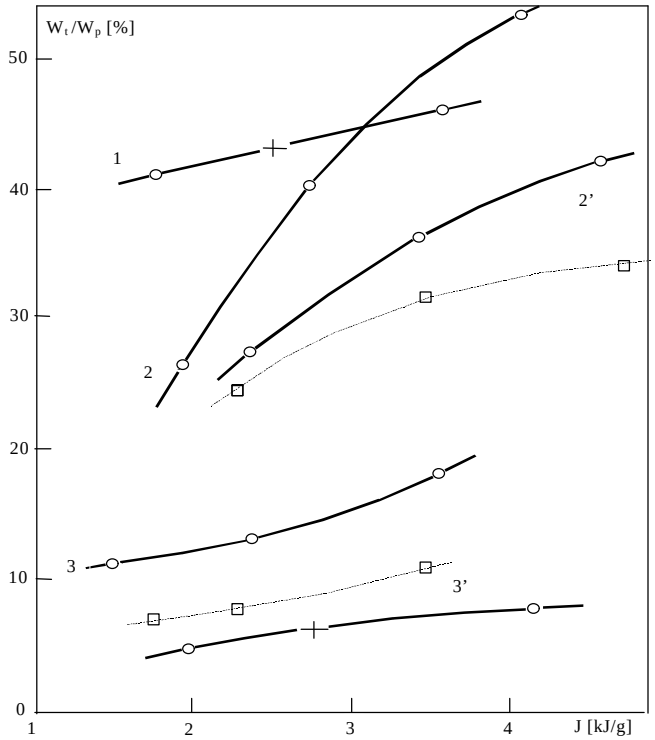

Figure 2: Heat losses in the microwave plasma generator. Full curves - experiments, broken curves - numerical simulations. (1) - FVS scheme without the diaphragm and with the plasma-chemical reactor, (2) - FVS scheme with the diaphragm and with the plasma-chemical reactor, (2') - FVS scheme with the diaphragm and without the plasma-chemical reactor (experiment and simulation), (3) - RVS scheme with the diaphragm and with the plasma-chemical reactor, (3') - RVS scheme with the diaphragm and without the plasma-chemical reactor (experiment and simulation).

the-wall for temperature in Fluent comprises two different laws: a linear law for the thermal conduction sublayer and a logarithmic law for the turbulent region. The minimum size of the grid cell near the wall was about 0.3 mm. The heating of the plasma was assumed to take place in an idealized uniform heat generation zone in the central region of the rotating flow. The pre-described heating zone length was 120 mm. Its diameter was varied, but was usually 26 mm. The metallic parts of the plasma generator were supposed to have a constant temperature of 300 K. On the cylindrical wall convective cooling with a heat transfer coefficient of 50 W m^{-2} K^{-1} and radiation cooling with an external emissivity of 0.8 were assumed. Test calculations showed that the most realistic flow pattern in the inlet regions was obtained in a 2D geometry when the discrete tangential gas inlet jets were simulated by fixing the rotating velocity in the cells next to the cylindrical wall and defining the appropriate mass sources for the same cells.

Figure 3(a) shows the streamlines, profiles of axial velocity and the temperature distribution for the FVS scheme, and Fig. 3(b) - for the RVS scheme. In these two modeling cases the heating zone (3.5 kW, length 0.14 m, diameter 44 mm) was in the center of the MW plasma torch quartz tube (1) (Fig. 1). Gas (nitrogen) enters tangentially into the discharge chamber (FVS scheme) or into the additional vortex chamber (RVS scheme). The initial velocity of the tangential gas jets was estimated from the measurements of the pressure drop and the gas consumption. In the two cases showed in Fig. 3 (a) and (b) the initial tangential velocities (and the gas consumption) are 100 m s^{-1} (1 g s^{-1}) and 225 m s^{-1} (1.5 g s^{-1}), respectively. It is easy to see (Fig. 3b) that the reverse vortex "compresses" the heat zone and protects the plasma torch walls from overheating. As it was initially supposed (Gutsol, 1997a; Kalinnikov and Gutsol, 1997), the main part of the plasma gas passes through the high temperature discharge zone and the size of recirculation zones are considerably reduced. In the FVS scheme (Fig. 3a), on the contrary, the main part of the incoming gas mixes with the hot recirculated flow and moves along the cylindrical quartz wall thus bypassing the discharge zone. The calculated energy losses for the appropriate cases are shown by the dots of the broken curves on Fig. 2 (curve 2' - for the FVS scheme, curve 3' - for the RVS scheme). A discrepancy between experimental and calculated results may occur due to the oversimplified description of the discharge zone, and probably also because of experimental errors. Nevertheless, this discrepancy is small enough to conclude that the energy losses might be reliably predicted for other electric discharges and in flames by employing numerical simulation models.

3. Radio Frequency Inductively Coupled Plasma Torch: Experiments and Simulation. The scheme of the RF inductive plasma torch with the reverse vortex flow is shown on Fig. 4. Plasma gas enters the discharge volume through tangential swirler (2). The water-cooled nozzle (1) prevents immediate exit of the plasma gas from the volume.

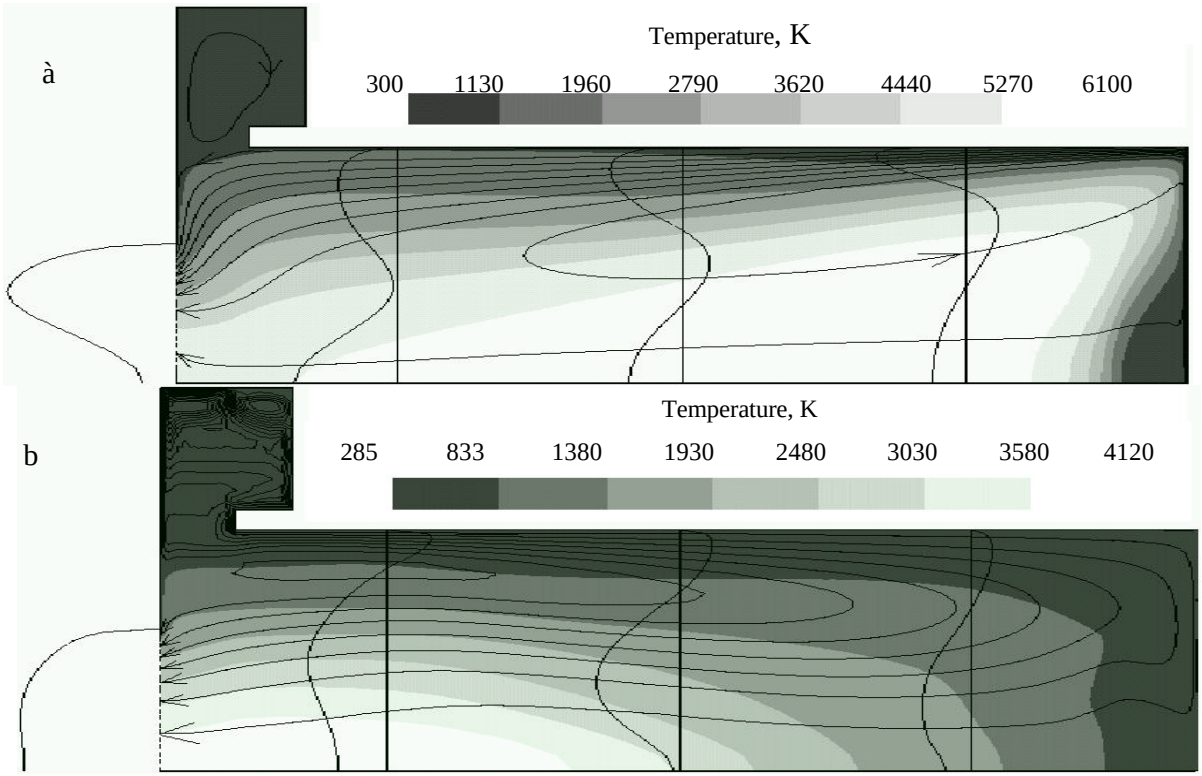

Figure 3: Temperature distribution, streamlines and profiles of axial velocity for three different cross-sections and for outlet of the MW plasma torches with conventional vortex flow (a) and with reverse vortex flow (b).

On the left side of the scheme the gas streamlines (5) are shown. The streamlines (7) of the gas and plasma in the radial plane are shown on the right side of the Fig 4. The discharge volume is restricted by the quartz tube (3). Water-cooled inductive coil (4) supplies RF electromagnetic energy, which is absorbed in the toroidal skin-layer (8) of the plasma fluid (9). Plasma leaves the discharge volume as a flow (6) through the nozzle (1).

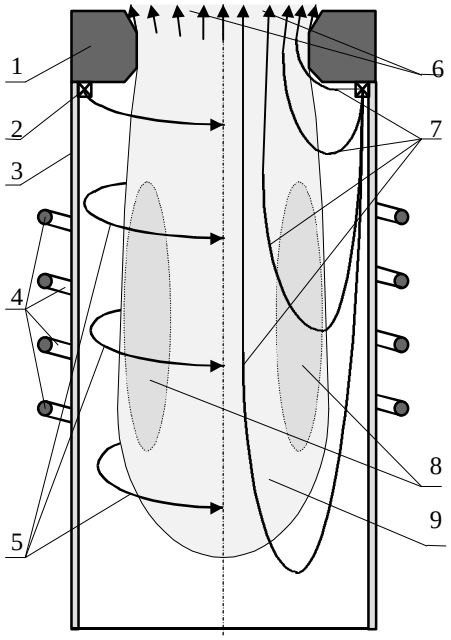

Fig. 4: Scheme of the inductively coupled RF plasma torch with RVS. 1 - water-cooled nozzle, 2 - tangential gas feeder for swirl flow formation, 3 - quartz tube, 4 - induction coil, 5 – gas streamlines, 6 – exit plasma flow, 7 - streamlines of the gas and plasma in the radial plane, 8 - skin layer, 9 - Inductively Coupled Plasma.

There is one fundamental difference between microwave plasma and ICP. In MW plasma there is a central hot zone with low flow velocity that acts as a stabilizing core producing active species and electrons. In ICP, the RF field energy is absorbed in a toroidal zone (8) around the center. The diameter of this zone determines the coupling efficiency of the energy transfer from the inductive coil (4) to the plasma (9). In reverse vortex flow, there is a significant negative radial flow component over the whole length of the active region. This radial flow should compress the toroidal skin-layer zone (8). Therefore, the stability of this setup should be lower than in MW or flame.

Preliminary experiments (Gutsol et al, 1999a) show that it is possible to obtain stable ICP plasma with reverse vortex flow configuration. The experiments were accomplished using a common RF power supply with a frequency of 2 MHz. The quartz plasma chamber has inner diameter of 75 mm. The 4-loop inductive coil has inner diameter of 90 mm and length of 100 mm. The distance between the 50 mm nozzle and the inductive coil is 70 mm. We have used argon as a plasma gas. In some experiments the admixture of nitrogen was used.

To compare the efficiencies of the RVS ICP and FVS ICP torches of the same geometry as plasma jet generators, total calorimetric measurements and numerical simulations were made using atmospheric pressure argon plasma. The FVS ICP torch geometry differs from the usually used one only by the nozzle ((1) on Fig. 4) on the plasma exit end.

In the calorimetric measurements and simulations we used a nozzle of 43 mm length and 25 mm smallest inner diameter, and a feeder of inner diameter of 72 mm that has four circular tangential inlets of 2 mm diameter. The quartz tube length was 380 mm and the center of the inductive coil was at 130 mm from the feeder side of the nozzle. After a preliminary study (Gutsol et al, 1999a) the plasma torch scheme was modified for the calorimetric measurements to provide water cooling of all surroundings including the quartz tube. The powers absorbed by the nozzle and the tube were measured separately. A stainless steel heat exchanger was mounted downstream of the plasma torch to measure the exhaust gas enthalpy. Measurement of the argon temperature after the heat exchanger indicated that heat loss after this point was negligible. We have measured the total radiation intensity at about 1.3 m distance from the plasma with a black-body surface absorber, and then calculated the total radiation loss with account of partial absorption by the non-transparent water-cooled parts of the plasma torch. The sum of all the measured losses (nozzle, tube, radiation and heat exchanger is equal to the total energy initially absorbed by the plasma from the inductive coil. The total discharge power W_d, measured with about 3% accuracy, was 55% - 75% of the plate power of the RF generator depending on the discharge regime and stabilization method. The plate power of the Soviet RF generator Â×È 11-60/1,76 was calculated by multiplying the anode voltage and anode current. The accuracy was poorer because of the low resolution of the monitoring devices. The repeatability of the discharge regime was not very high either, as the final adjusting of the generator-discharge system could be made only after the discharge ignition.

The experiments with a FVS ICP in the geometry with the contracted plasma exit have shown the extremely high stability of this discharge. It is possible to change the RF generator power by an order of magnitude with the same argon mass flow, and the discharge remains stable, only its brightness and volume change. Considering a modeling result for this discharge (Fig. 5), the reason of the high stability becomes obvious. The gas flows mostly around the discharge and cools it mainly through the "surface" (conductive cooling). The discharge "lives its own life" absorbing energy from the electromagnetic field. When the RF power is increased, the stronger Lorentz force pulls more gas from the circumventing flow towards the skin region. Moreover, the plasma expands due to the increased power, and as a result the gas temperature in the circumventing flow increases and the gas expands thermally, partially mixing with the plasma. Thus, the result of power increment is electromagnetic and thermodynamic "pumping" of gas through the plasma region (convective cooling).

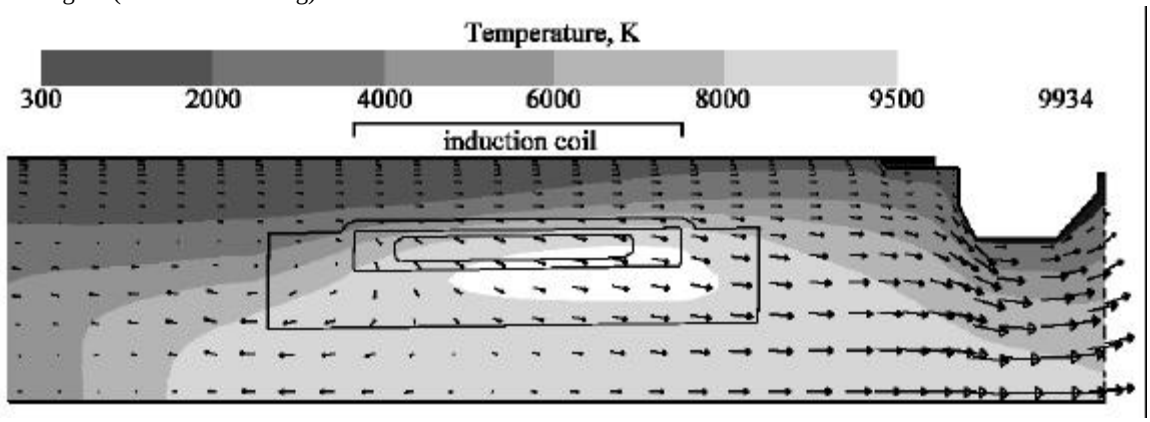

Fig. 5: Simulation results for the common ICP in the new plasma torch geometry. Temperature distribution, velocity vectors in the axial plane, zones of heating and negative radial momentum due to Lorenz force (the largest one - 3.6×10^7 W/m^3, 150 N/m^3; the middle one - 1.08×10^8 W/m^3, 450 N/m^3; the small one - 1.62×10^8 W/m^3, 625 N/m^3).

The power characteristics of the FVS ICP, such as the dependence of the average plasma jet enthalpy on the plate power and the dependence of the plasma torch efficiency on the discharge power (Fig. 6) are typical. Here the plasma

torch efficiency η is the ratio of the plasma jet power W_j (we assume that the power of the plasma jet is equal to the power absorbed by the heat exchanger) to the total discharge power W_d: $\eta = W_j/W_d$. Plate power increase under a constant argon mass flow rate results in an increase of the average plasma jet enthalpy from 0.8 kJ/g to 3 kJ/g. Argon mass flow rate increase under a constant plate power results in a decrease of the average plasma jet enthalpy. The plasma torch efficiency drops with the growth of the discharge power and with the decrease of argon mass flow rate (Fig. 6). Thus, the FVS ICP is able to generate a high enthalpy plasma jet with low efficiency or a low enthalpy plasma jet with rather high efficiency. It is possible to see in Fig. 6a that the simulation results are in a reasonable agreement with the experimental results.

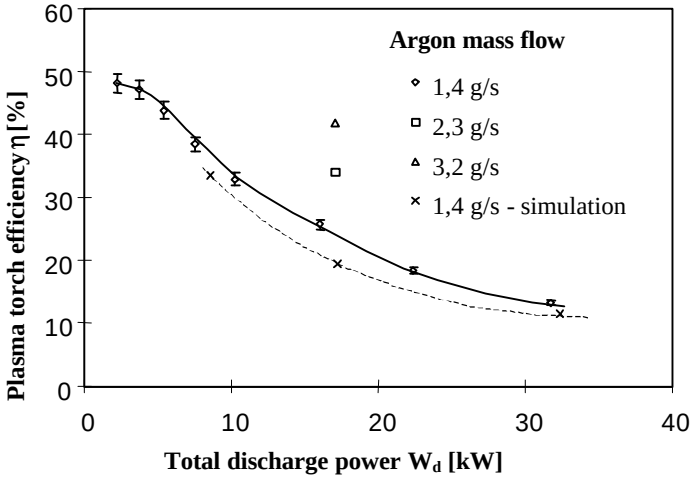

Fig. 6: Argon FVS ICP. Dependence of the plasma torch efficiency on the total discharge power for different argon mass flow. Experimental and simulation.

Considering the stability of the RVS ICP, the power threshold for its existence is much higher than for FVS ICP. The plasma torch efficiency for the RVS (Fig. 7) also drops with the growth of the discharge power and the decrease of the gas flow rate, though η reaches a higher level than in the FVS ICP.

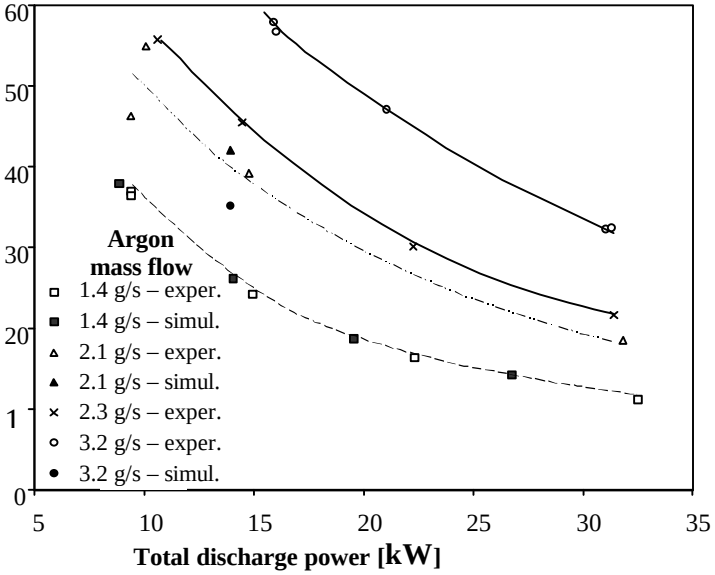

Fig. 7: Argon RVS ICP. Dependence of the plasma torch efficiency on the total discharge power for different argon mass flow. Experimental and simulation.

The average enthalpy of the argon plasma jet generated by the RVS ICP is higher than 2 kJ/g in all cases. It does not grow only with the plate power, but also with the argon mass flow rate, which is extremely unusual for any type of discharge. It is possible to understand the reason for this phenomenon by looking at the result of the numerical simulation in Fig. 8. The gas flows mostly through the active discharge zone and after that its enthalpy rises to a very high and approximately constant level. An additional recirculation zone is formed in the closed part of the discharge

tube due to the Lorentz force. Probably it is this recirculation that creates the plasma "tail", observed in some conditions during the preliminary study (Gutsol et al, 1999a), and results as some additional heat and radiation losses. (The fraction of the radiation losses in the total energy balance of the RVS ICP torch varied in a wide range: from 8% to 32%.) The increase of the plasma gas flow results in shrinking of the additional recirculation zone and the plasma volume. This leads to a significant reduction of heat losses via the quartz tube and radiation, so the average plasma jet enthalpy increases. This phenomenon indicates that the RVS ICP torch is capable of generating a high enthalpy plasma jet with a high efficiency. This property is very useful in various applications. Fig. 6b also shows that the modeling results for the plasma jet generation efficiency of the RVS ICP torch was in good agreement with experiments. A large discrepancy between the experimental curve and the simulated result can be seen only beyond the experimentally observed range of discharge stability (see data for the argon mass flow 3.2 g/s and 14 kW power).

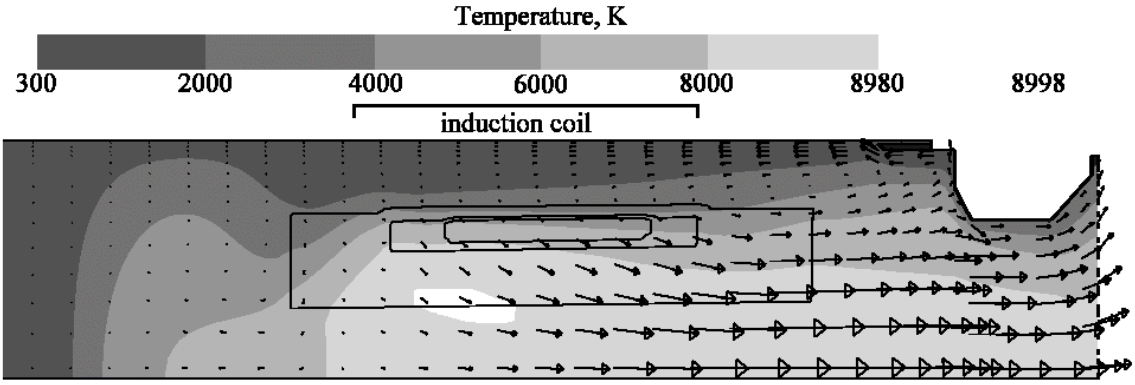

Fig.8: Simulation results for the reverse vortex stabilized ICP. Temperature distribution, velocity vectors in the axial plane, zones of heating and negative radial momentum due to Lorenz force (the largest one - 3.68×10^7 W/m^3, 150 N/m^3; the middle one - 1.1×10^8 W/m^3, 450 N/m^3; the small one - 1.65×10^8 W/m^3, 625 N/m^3).

For numerical simulations we used the FLUENT program, version 4.47. To account for turbulence the Reynolds Stress Model (RSM) with non-equilibrium wall function and with account of directional diffusivity of turbulence was used. The domain shape was equal to the inner torch region. Non-uniform and non-rectangular grid contains 226×30 cells. On the figures 5 and 8 the plasma torch is shown without the bottom part. Induction coil length is 100 mm, the torch radius is 37.5 mm. Argon (3.77 g/s = 127 Nl/min) comes into the discharge volume tangentially near the bottom (in common ICP) with the velocity 40 m/s, or near the nozzle (in RVS ICP) with the velocity 83.4 m/s.

One can see that the hot zone (T > 6000 K) of the FVS ICP is very large due to the intensive recirculation. In the RVS ICP the hot zone is compressed by the incoming cold gas. The maximum temperature for the RVS ICP is considerably lower. The same tendencies were observed in the simulation of the microwave (MW) discharge (see above). The heat efficiency of these two simulated plasma torches are 39 % for the FVS and 54 % for the RVS with approximately the same energy input 5.6 kJ/g (plasma power 21.5 kW).

According to the modeling, some recirculation also takes place near the tangential feeder (Fig. 8), which results as an intensive heat flux to the feeder side of the nozzle. This result is in contradiction to our insight of the flow close to the nozzle surface (Gutsol, 1997b) (See also Fig. 4). We suppose that a surface gas flow directed to the nozzle axis should exist near the swirl feeder that should protect the nozzle from overheating. In practice, the measured nozzle heat loss (6% -16%) was always approximately half of the simulated value. The reason of this contradiction may be in too coarse computational grid near the nozzle surface. Unfortunately, further grid refining did not seem reasonable because of the sharp increment of the computing time. (With the non-uniform and non-rectangular grid of 226x30 cells, computing time for one simulation was some hours on an Alpha Station 600 5/333.)

Comparing the obtained plasma jet generation efficiency (up to 48 % for the FVS and 58 % for the RVS) of the studied argon RF plasma torches with a water-cooled nozzle with reliable data for other argon ICP torches (about 55% for the torch without a nozzle but with a water-cooled probe for material feeding (Merkhouf and Boulos, 1999); up to 45% in paper of Reed (1961); up to 37% in the papers cited in the article (Goykhman and Gol'dfarb, 1977), it becomes clear that the plasma jet generation efficiency of this RVS ICP torch is rather high. This is a promising property for those torches where the nozzle is a necessary design part, for example, in the sources of supersonic plasma jets (Hollenstein et al, 1999).

From the application point of view, probably the most promising property of the reverse vortex flows is the possibility to inject an additional axial flow from the closed end of the system without substantially disrupting the flow pattern (simulation results in Fig. 9). Our experiments showed that the axial argon flow could be as strong as the main swirl argon flow without extinguishing the discharge. The calorimetric measurements of a similar regime gave the next results: at 49 kW plate power, 2.29 g/s argon mass flow through the tangential feeder and additional 0.85 g/s of nitrogen mass flow through the axial tube, the discharge absorbed 36.46 kW (74.4 % of plate power). With 48.4 % efficiency, it generates a plasma jet with average enthalpy of 5,62 kJ/g. This corresponds approximately to 6000K temperature for the

given mixture of an argon and nitrogen. Therefore, it may be possible to insert large quantities of material (gaseous or disperse) into plasma treatment in the active zone. According to our insight the treated products should not interact with the plasma torch wall significantly. This property may open new opportunities in plasma technology, as the lack of such properties in traditional RF discharges restricts their applications in plasma chemistry and technology (McKelliget and El-Kaddah, 1988).

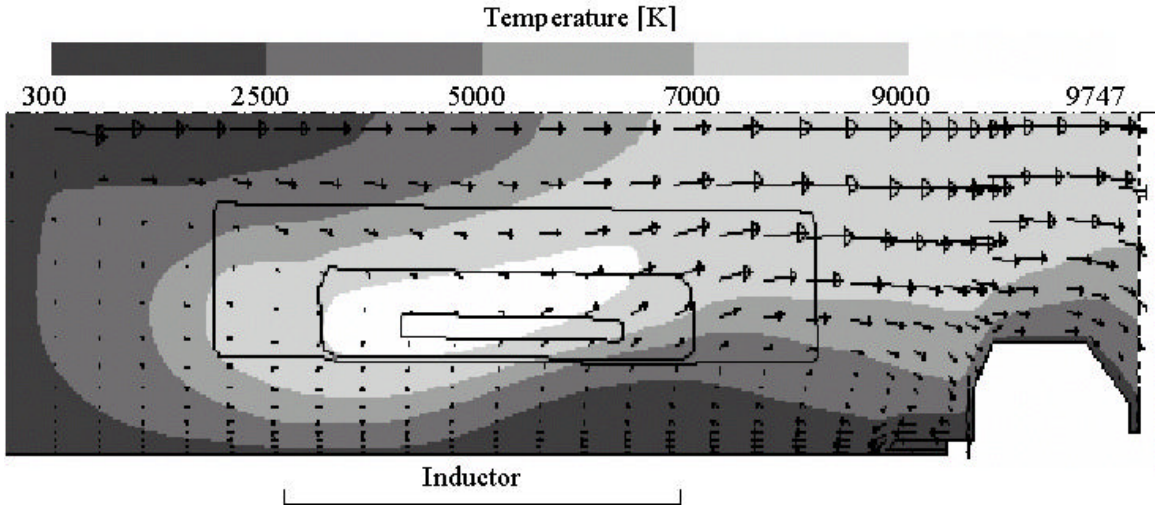

Fig.9: Simulation results for the reverse vortex stabilized ICP with additional axial flow. Total discharge power: 21 kW, argon mass flow: 2.1 g/s (reverse vortex flow) + 0.7 g/s (additional axial flow). Temperature distribution, velocity vectors in the axial plane, zones of heating and negative radial momentum due to Lorenz force (the largest one - 3.68×10^7 W/m^3, 150 N/m^3; the middle one - 1.1×10^8 W/m^3, 450 N/m^3; the small one - 1.65×10^8 W/m^3, 675 N/m^3).

4. Conclusion. Experimental investigations and numerical simulations show that RVS is very promising for different plasma technology applications. A discrepancy between experimental and calculated results was small enough to conclude that the energy losses might be reliably predicted on the design stage of electrodeless plasma torches with the both types of vortex stabilization.

REFERENCES

GOYKHMAN, V. KH. AND GOLDFARB, V. M. High-frequency inductive thermal discharge. In *Plasmokhimicheskie Reaktsii i Protsessy* (*Plasma Chemical Reactions and Processes*), Nauka, Moscow (1977), 231-278. IN RUSSIAN.

GUTSOL, A. F. Plasma processing of fluoride solutions of refractory rare metals. *Khimiya vysokikh energiy (High Energy Chemistry) 29* (1995), 373-376.

GUTSOL, A. F. Method for the flow system formation. *Patent 2086812 RU, I.Cl*^{6} *F 15 D 1/00. - No. 95112323/06; Appl. 18.07.95; Publ. 10.08.97, Izobreteniya (Inventions)*, (1997a) No. 22, P. 344. IN RUSSIAN

GUTSOL, A. F. The Ranque effect. *Physics - Uspekhi 40* (1997b), 639-658.

GUTSOL, A., AND BAKKEN, J. A. New Vortex Method of Plasma Insulation and Explanation of the Ranque Effect. *J.Physics D: Applied Physics 31* (1998), 704 - 711.

GUTSOL, A., LARJO, J., AND HERNBERG, R. RF Inductive Plasma Torch with Reverse Vortex Flow Stabilization. In *Proceedings of the 14th International Symposium on Plasma Chemistry*, (Prague, August 2 - 6, 1999a), Vol. 1, 227 - 231.

GUTSOL, A., LARJO, J., AND HERNBERG, R. The Effect of Turbulence Model on the Simulation of Gas Flow in ICP. In *Proceedings of the 14th International Symposium on Plasma Chemistry*, (Prague, August 2 - 6, 1999b), Vol. 1, 275 - 280.

HOLLENSTEIN, M., RAHMANE, M. AMD BOULOS, M. I. Aerodynamic Study of the Supersonic Induction Plasma Jet. In *14th International Symposium on Plasma Chemistry*, (Prague, August 2-6, 1999), Vol. 1. 257 - 261.

KALINNIKOV, V. T., AND GUTSOL, A. F. A New Efficient Method of Insulating High-Temperature and Reacting Systems and the Ranque Effect. *Physics – Doklady 42*, (1997), 179 - 181.

MCKELLIGET, J. W. AND EL-KADDAH, N. The effect of coil design on materials synthesis in an inductively coupled plasma torch. *J. Appl. Phys.* 64, (1988), 2948 - 2954

MERKHOUF, A. AND BOULOS, M. I. Experimental validation for an integrated model of the induction plasma generation system. In *Proceedings of the 14th International Symposium on Plasma Chemistry*, (Prague, August 2 - 6, 1999), Vol. 1, 421 - 426.

REED, T. B. Induction-Coupled Plasma Torch. *J. Appl. Phys.* 32, (1961), 821.